

A Massive Core in Jupiter Predicted From First-Principles Simulations

B. Militzer

*Departments of Earth and Planetary Science and of Astronomy,
University of California, Berkeley, CA 94720, USA.*

W. B. Hubbard

Lunar and Planetary Laboratory, The University of Arizona, Tucson, AZ 85721, USA.

J. Vorberger

Department of Physics, University of Warwick, Coventry CV4 7AL, UK.

I. Tamblyn and S.A. Bonev

*Department of Physics and Atmospheric Science,
Dalhousie University, Halifax NS B3H 3J5, Canada.*

Hydrogen-helium mixtures at conditions of Jupiter’s interior are studied with first-principles computer simulations. The resulting equation of state (EOS) implies that Jupiter possesses a central core of 14 – 18 Earth masses of heavier elements, a result that supports core accretion as standard model for the formation of hydrogen-rich giant planets. Our nominal model has about 2 Earth masses of planetary ices in the H-He-rich mantle, a result that is, within modeling errors, consistent with abundances measured by the 1995 Galileo Entry Probe mission (equivalent to about 5 Earth masses of planetary ices when extrapolated to the mantle), suggesting that the composition found by the probe may be representative of the entire planet. Interior models derived from this first-principles EOS do not give a match to Jupiter’s gravity moment J_4 unless one invokes interior differential rotation, implying that jovian interior dynamics has an observable effect on the measured gravity field.

I. INTRODUCTION

The discovery of over two hundred extrasolar planets resembling the giant planet Jupiter in mass⁴⁰ and composition⁵ has raised fundamental questions about the origin and inner structure of these bodies. Establishing the existence of a dense core in Jupiter is vital for understanding the key processes of planetary formation. An observed correlation between the metallicity of the parent star and the likelihood of giant planets orbiting it¹⁰ may indicate that an initial core aggregated from solid planetesimals triggers the gravitational collapse of nebular gases to form giant planets²⁴, or alternatively, increased metallicity enhances the direct collapse of giant planets from the nebula²¹. Current planetary models^{32,33} predict only a very small core between 0 and 7 Earth masses (M_E) for Jupiter, lending support to core-accretion theories with comparatively small cores²⁸, late-stage core erosion scenarios¹², or suggesting that jovian planets are able to form directly from gases without a triggering core⁴. Using first-principles simulations for hydrogen-helium mixtures at high pressure, we show here that Jupiter possesses a significant central core of $16 \pm 2 M_E$ of heavier elements, a result that supports core accretion as the standard model for formation of hydrogen-rich giant planets. In our model, Jupiter’s mantle, defined as the H-He-rich outer layers, shows no enrichment of heavier elements, indicating that compositional measurements from the 1995 Galileo Entry Probe mission may be representative of most of the planet. The derived interior models also pro-

vide the first evidence that Jupiter’s interior does not rotate as a solid body because no match to Jupiter’s gravity moment J_4 is obtained unless one invokes interior differential rotation, implying that jovian interior dynamics have an observable effect on the measured gravity field.

While laboratory techniques cannot yet probe deep into Jupiter’s interior (reaching pressures $P \sim 100$ – 1000 GPa and temperatures $T \sim 10000$ K), advances in first-principles computer simulation techniques have made it possible to characterize the equation of state (EOS) of hydrogen-helium mixtures for the entire planet. The determination of the EOS, in combination with the modeling reported here, enables us to more precisely specify Jupiter’s mantle metallicity and core mass.

II. SIMULATION METHODS

All density functional molecular dynamics (DFT-MD) simulations were performed with either the CPMD code⁽⁸⁾ using local Troullier-Martins norm-conserving pseudopotentials or with the Vienna *ab initio* simulation package¹⁹ using the projector augmented-wave method³. The nuclei were propagated using Born-Oppenheimer molecular dynamics with forces derived from the electronic ground state. Simulations with thermally excited electronic states did not yield any significant correction to the EOS in Jupiter’s interior. Exchange-correlation effects were described by the generalized gradient approximation²⁷. The electronic wavefunctions were expanded

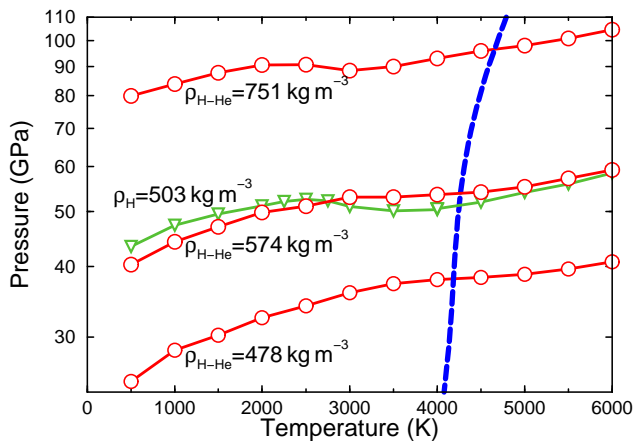


FIG. 1: Isochores derived from DFT-MD simulations of H-He mixtures (circles, $Y=0.2466$) and pure hydrogen (triangles). Results for mixtures predict a positive Grüneisen parameter, $(\partial P/\partial T)|_V > 0$, along Jupiter’s isentrope (dashed line) predicting the planet to be isentropic and fully convective.

in a plane-wave basis with a 35-50 Hartree energy cutoff. The simulations were run for 2 picoseconds with time steps ranging between 0.2 and 0.8 femtoseconds. We performed well over a hundred separate DFT-MD simulations on a non-uniform grid in density and temperature ranging from $\rho=220 - 6006 \text{ kg m}^{-3}$ and 500 - 20000 K. At lower densities, we used classical Monte Carlo simulations with fitted potentials³¹, which are in good very agreement with the SC EOS.

All simulations were performed with 110 hydrogen and 9 helium atoms in periodic boundary conditions. The initial simulations were performed with Γ point sampling of the Brillouin zone only. Further simulations with uniform grids of up to $4 \times 4 \times 4$ k-points exhibited a correction to the pressure in the metallic regime. This correction slowly increases with density, eventually reaching -1.6% at conditions of Jupiter’s core. Finite size effects were further analyzed by Vorberger et al.³⁸. The isentropes were derived from a thermodynamically consistent fit to the free energy using an approach that was described in detail in Ref.²³.

DFT-MD predicts a continuous transition from the molecular to a dissociated regime in fluid hydrogen as function of pressure^{37,38}, which is consistent with quantum Monte Carlo simulations⁹. The dissociation transition in dense hydrogen is driven by the increasing overlap of molecular orbitals. At sufficiently high compression, Pauli exclusion effects trigger a delocalization of the electronic charge²², the band gap closes^{37,38}, the conductivity increases, the protons are no longer paired, and eventually the system assumes a metallic state¹⁸. As the temperature of the fluid increases, this transition occurs at lower pressures due to stronger collisions. When helium is added to dense hydrogen, it localizes the electronic charge because of its stronger binding. It dilutes the hydrogen subsystem by reducing overlap of molecu-

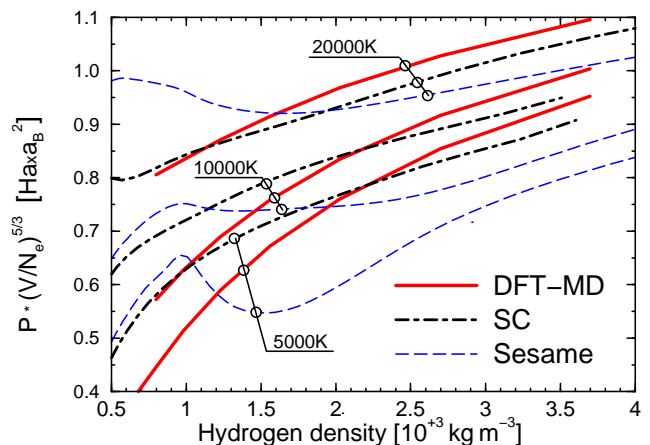


FIG. 2: Comparison of the DFT-MD EOS with the SC and Sesame models. Three isotherms for pure hydrogen are shown in the metallic regime at high pressure. P is scaled by the volume per electron to the power $\frac{5}{3}$ to remove most of the density dependence.

lar orbitals, increasing the stability of hydrogen molecules compared to pure hydrogen at the same P and T ³⁸.

While the DFT-MD EOS has a positive compressibility for all P and T , such that $(\partial P/\partial \rho)_T > 0$ (where ρ is the mass density), the method predicts a negative Grüneisen parameter, equivalent to $(\partial P/\partial T)_\rho < 0$, for the dissociation region of pure hydrogen^{37,38}. A negative Grüneisen parameter would introduce a convection barrier into Jupiter’s mantle. However, Figure 1 demonstrates that in a H-He mixture, the region where $(\partial P/\partial T)_\rho$ is negative occurs at higher pressures and significantly lower temperatures than are present in Jupiter’s interior. Consequently, Jupiter’s mantle is predicted to be fully convective and isentropic.

III. INTERIOR MODELS

Were Jupiter of exactly solar composition and all its magnesium-silicates and iron together with the abundant hydrides CH_4 , NH_3 , and H_2O concentrated in a dense core, considering recent reductions in the solar C and O abundances, its core mass would only comprise about $3 M_E$ ^{11,29,30}. The core mass thought to trigger nebular collapse is several times larger²⁴. Detection of a central core with a resolution of a few M_E , only 1% of Jupiter’s total mass of $318 M_E$, places stringent demands on the accuracy of the hydrogen-helium EOS. We show in this Letter that an EOS based on density functional molecular dynamics (DFT-MD) differs from the previous Saumon-Chabrier-Van Horn (SC) EOS^{7,32} by considerably more than one percent.

Figure 2 compares the DFT-MD results for pure H with the SC EOS. The SC model relies on analytical techniques that describe hydrogen as an ensemble of stable molecules, atoms, free electrons, and protons. Approx-

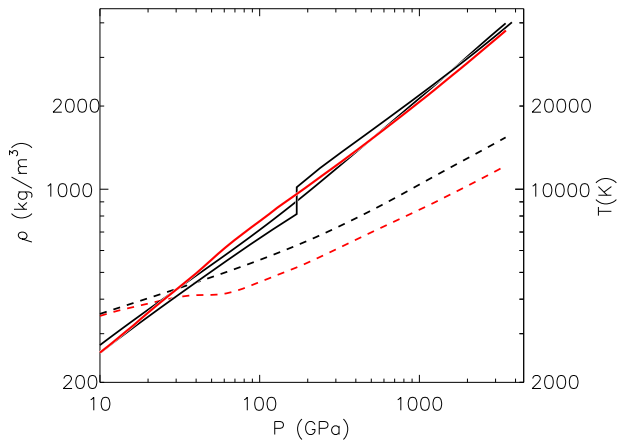


FIG. 3: Comparison of the resulting Jupiter models. Solid curves show mass density (left-hand ordinate) and dashed curves show temperature T (right-hand ordinate), as a function of pressure P . In contrast to Fig. 2, the DFT-MD (red line) and the SC models have differing chemical compositions and temperatures at each pressure. The outermost layers at $P < 100$ GPa make about 90 percent of the contribution to the gravity moment J_4 . The black curves show two models based on the smoothed and discontinuous versions of the SC EOS.

mations are made to characterize their interactions. Conversely, with DFT-MD one simulates a fully interacting quantum system of over a hundred electrons and nuclei. The isotherms shown in Fig. 2 specify the EOS in the inner regions of Jupiter where hydrogen is metallic. Due to the lack of experimental data at this density, predictions from chemical models including the Sesame database²⁰ vary substantially. The DFT-MD method obtains higher densities than the SC EOS for much of the pressure range characteristic of the interior of Jupiter. This has great influence on the predicted core mass. Moreover, DFT-MD predicts a continuous molecular-to-metallic transition while the original SC EOS model predicts this transition to be of first order, which introduced the possibility of having different chemical compositions in the inner and outer layers of Jupiter. Guillot et al.¹³ showed that having flexibility to redistribute materials allows one to make a coreless model for Jupiter while typical models with constant chemical composition in the mantle predict a core of about $7 M_E$ when the SC EOS is used. Conversely, our DFT-MD EOS predicts Jupiter’s mantle to be isentropic, fully convective, and of constant chemical composition. As we show below, the mantle metallicity is so low that compositional gradients would be unlikely to change this conclusion.

Jupiter isentropes from different models are compared in Fig. 3. The chemical composition corresponding to each isentrope was determined by adding ~ 0.7 mass percent of CH_4 , NH_3 , and H_2O (collectively called “planetary ices”²⁶), using ideal mixing, to the mixture of H and He considered here. The adequacy of the ideal-mixing ap-

proximation was verified by several H-He simulations at relevant pressures and temperatures with “guest atoms” of C, N or O. The DFT-MD EOS was derived with a single H-He composition, corresponding to 9 He atoms per 110 H atoms, or a He mass fraction $Y = 0.2466$, to be contrasted with the Jovian atmospheric He mass fraction measured by the Galileo entry probe, $Y = 0.2315 \pm 0.0061$ ³⁶. The DFT-MD isentrope was then perturbed to the probe He abundance by using ideal mixing with a pure He density at the same T and P , synthesized from separate DFT-MD simulations for pure helium²³. As can be seen in Fig. 3, DFT-MD implies lower temperatures in the deep jovian interior in isentropic models, further contributing to generally increased density with respect to SC models. The high density requires us to adopt $Y = 0.2315$ throughout the mantle in order to allow a non-negative planetary ice fraction. Figure 3 compares the original discontinuous SC EOS as well as the smoothed SC EOS version that we use in Figs. 2 and discuss below.

The DFT-MD EOS yields a significant revision of the interior structure of Jupiter. The resulting model predicts a large central core of 16 Earth masses and a low metallicity for the mantle while models based on the SC EOS imply a small core and a much higher metallicity in the mantle, comprising some tens of Earth masses of elements heavier than H and He^{13,33}. DFT-MD based models predict that the planetary ices were primarily incorporated into a massive solid core and depleted gaseous nebula. Conversely, models based on the SC EOS imply that planetary ices were largely accumulated along with the nebular hydrogen and helium when Jupiter formed. Figure 3 shows that the Jupiter model based on the DFT-MD EOS is about 5% denser than the model based on the smoothed SC EOS over the pressure range $30 \text{ GPa} < P < 300 \text{ GPa}$, which spans about 30% of the mass of Jupiter, while it is a few percent less dense at deeper layers. The Galileo Probe found abundances of CH_4 , NH_3 , and H_2O (at the deepest level) corresponding to at most about $5 M_E$ of planetary ices if extrapolated to the entire mantle. Our nominal model has about $2 M_E$ of planetary ices in the mantle. Given the cumulative uncertainties of the DFT-MD EOS and the planetary ices EOS, the nominal model is consistent with such an extrapolation of the Galileo measurements.

If Jupiter formed in a region of the solar nebula where temperatures were too low for H_2O to be in the gas phase, it would follow that a primordial core would include most of the H_2O in solid form, and that accreted nebular gas would accordingly be depleted in H_2O . This is consistent with the last model in Table I. We estimate that the non-H-He component of Jupiter’s mantle comprises $2 \pm 2 M_E$, and Jupiter’s dense core comprises $16 \pm 2 M_E$. The error bars include systematic and statistical uncertainties in the DFT-MD EOS. The dense core is modeled as rock and H_2O in solar proportions, but could for example include $\sim 5 M_E$ of sedimented He for an initial $Y = 0.25$. Simulation parameters were chosen in order to reach an accuracy of 1% within the DFT method. A uniform 1%

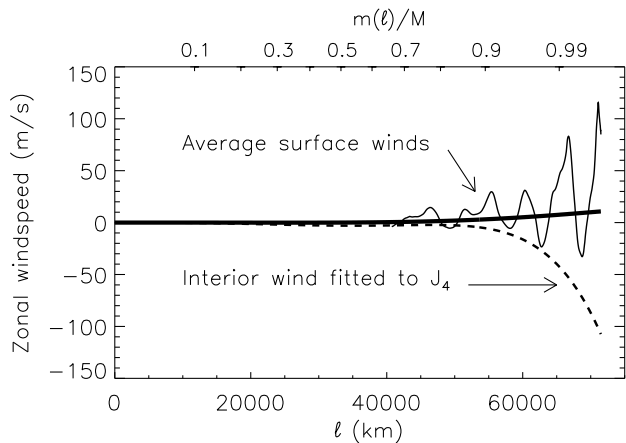


FIG. 4: Jupiter’s zonal wind speeds as a function of l , the distance from the rotation axis. The oscillating curve shows an average of northern and southern hemisphere surface zonal winds as determined by cloud motions; the heavy solid curve shows a fit of the surface winds with an eighth-order polynomial in l . The dashed curve shows our preferred rotation model that provides a match to Jupiter’s low-degree gravitational moments with the DFT-MD EOS. The upper abscissa gives the relative mass enclosed within a cylinder of radius l .

alteration of the pressure changes the core mass by $1 M_E$. An earlier Jupiter model based on a completely different set of DFT-MD EOS results for pure hydrogen³⁸ yielded a core mass that differed by $2 M_E$. We use this difference to estimate the uncertainties of our predictions.

An acceptable model of Jupiter’s interior must match the observed constraints of the planet’s mass, equatorial radius at a standard pressure of 1 bar, and the observed multipole moments J_2 , J_4 , J_6 of the gravity field normalized to the equatorial radius. Jupiter’s multipole moments are primarily a response to the planet’s rotation, and the higher-order moments can be strongly affected by nonuniform rotation. Traditional models of Jupiter’s interior structure and external gravity have assumed solid-body rotation equal to the rotation rate of the magnetic field (the corresponding rotation period is 9:55:29.7 hours, stable over decades³⁴). Our model calculations find the axially-symmetric mass density through a self-consistent field (SCF), calculated to fourth order in the rotational distortion^{14,16}. We incorporate differential rotation on cylinders to the same order as the SCF. Table I shows that models with solid-body rotation and the DFT-MD EOS predict a $|J_4|$ that is seven standard deviations larger than the observed $|J_4|$. The error bar of J_4 has decreased by about a factor three¹⁷ with respect to earlier determinations⁶. As predicted by theory¹, reduced $|J_4|$ is associated with a more rapid decrease of density with radius in the pressure range 1 to 100 GPa. However, we have no physical justification for making ad hoc modifications to the $P(\rho)$ relation in this pressure range. Since we have a fully convective mantle in

our model, we cannot match J_4 by distributing helium unevenly in an upper and lower mantle layer, which is one major difference compared to earlier models e.g.³³. Because the mantle metallicity is so low, neither can we redistribute mass by invoking composition gradients. It is more plausible that Jupiter’s J_4 is affected to a measurable extent by zonal winds in this pressure range. We bring the calculated J_4 into agreement without appreciably changing any other parameters of the model by assuming the zonal wind profile shown in Fig. 4 (preferred model in Table I). The shallower part of the wind profile could be adjusted further to force better agreement with J_6 , but such a refinement lies outside the scope of this paper. In that regard, we note a recent paper² that models deep zonal flows in Saturn by fitting gravity data.

To ensure that numerical errors do not play any role in the mismatch of J_4 , we checked our calculations with two independent theories for rotationally-distorted models of Jupiter. The standard theory³⁹ solves iteratively for the shape of level surfaces to third order in the rotational perturbation, sufficient to calculate J_2 to a relative precision of 10^{-3} , J_4 to about 10^{-2} , and J_6 to about 10^{-1} . The results agree well with the more accurate SCF method.

It has been shown¹⁵ that high-order Jupiter gravity harmonics are sensitive to interior dynamics in the outermost planetary layers at pressures less than about 10 GPa. There is no significant uncertainty in the hydrogen EOS at these pressures, which are accessible to experiment²⁵. This is why we investigated whether the DFT-MD EOS, coupled with plausible models of Jovian mantle dynamics, could reproduce the observed Jovian gravity field. According to the Poincaré-Wavre theorem³⁵, the requirement that there be a single pressure-density relation (barotrope) within Jupiter is a necessary and sufficient condition that deep windspeeds be constant on cylindrical surfaces of constant l . Mapping the observed windspeeds onto such cylinders and then fitting the implied centrifugal potential with a polynomial to degree eight in l , we obtain the heavy curve in Fig. 4. When this fit is incorporated in the SCF calculations, we find insignificant shifts in the predicted values of J_n ($n = 2, 4, 6$), although the winds could affect higher-order Jupiter gravity components¹⁵. The assumed retrograde deep zonal wind has negligible effect on Jupiter’s total spin angular momentum, reducing the latter by only 0.06% with respect to a windless model.

New observational data concerning these theoretical predictions are expected from the NASA mission Juno. Juno is a low-periapse Jupiter orbiter that will return unprecedented data on Jupiter’s high-order gravitational and magnetic fields during 2016. It may present the first direct evidence of deep interior zonal flows in Jupiter proposed here.

Acknowledgments

B.M., W.B.H., and J.V. acknowledge support from NASA and NSF. I.T. and S.A.B. acknowledge support

from NSERC, and computational resources from IRM (Dalhousie) and Westgrid. We thank A. Burrows and J. Fortney for comments.

-
- ¹ Anderson, J. D., Hubbard, W. B., & Slattery, W. L. 1974, *Astrophys. J. Lett.*, 193, L149
- ² Anderson, J. D., & Schubert, G. 2007, *Science*, 317, 1384
- ³ Blöchl, P. E. 1994, *Phys. Rev. B*, 50, 17953
- ⁴ Boss, A. P. 2007, *Astrophys. J.*, 661, L73
- ⁵ Burrows, A., Hubeny, I., Budaj, J., & Hubbard, W. 2007, *Astrophys. J.*, 661, 502
- ⁶ Campbell, J. K., & Synnott, S. P. 1985, *Astron. J.*, 90, 364
- ⁷ Chabrier, G., Saumon, D., & Potekhin, A. Y. 2006, *J. Phys. A: Math. Gen.*, 39, 4411
- ⁸ CPMD. 1990-2006, copyright IBM Corp, MPI für Festkörperforschung Stuttgart 1997-2001.
- ⁹ Delaney, K. T., Pierleoni, C., & Ceperley, D. M. 2006, *Phys. Rev. Lett.*, 97, 235702
- ¹⁰ Fischer, D. A., & Valenti, J. 2005, *Astrophys. J.*, 622, 1102
- ¹¹ Grevesse, N., & Sauval, A. J. 1998, *Space Science Reviews*, 85, 161
- ¹² Guillot, T., *et al.* 2004, *Jupiter*, ed. W. M. F. Bagenal, T.E. Dowling (Cambridge Univ. Press, Cambridge)
- ¹³ Guillot, T., Gautier, D., & Hubbard, W. B. 1997, *Icarus*, 130, 534
- ¹⁴ Hubbard, W. B. 1982, *Icarus*, 52, 509
- ¹⁵ —. 1999, *Icarus*, 137, 357
- ¹⁶ Hubbard, W. B., Slattery, W. L., & DeVito, C. L. 1975, *Astrophys. J.*, 199, 504
- ¹⁷ Jacobson, R. A. 2003, JUP230 orbit solution http://ssd.jpl.nasa.gov/?gravity_fields_op
- ¹⁸ Johnson, K., & Ashcroft, N. W. 2000, *Nature*, 403, 632
- ¹⁹ Kresse, G., & Hafner, J. 1993, *Phys. Rev. B*, 47, 558
- ²⁰ Lyon, S. P., and Johnson, J. D., 1992, eds, Los Alamos National Laboratory EOS database, report LA-UR-92-3407, table Hydr5251.
- ²¹ Mayer, L., Lufkin, G., Quinn, T. & Wadsley, J. 2007, *Astrophys. J.*, 661, L77
- ²² Militzer, B. 2005, *J. Low Temp. Phys.*, 139, 739
- ²³ —. 2008, submitted to *Phys. Rev. B*, arXiv:0805.0317
- ²⁴ Mizuno, H. 1980, *Progress of Theoretical Physics*, 64, 544
- ²⁵ Nellis, W. J. 2002, *Phys. Rev. Lett.*, 89, 165502
- ²⁶ Nellis, W. J. *et al.* 1997, *J. Chem. Phys.*, 107, 9096
- ²⁷ Perdew, J. P., Burke, K., & Ernzerhof, M. 1996, *Phys. Rev. Lett.*, 77, 3865
- ²⁸ Pollack, J. *et al.* 1996, *Icarus*, 124, 62
- ²⁹ Prieto, C. A., Lambert, D. L., & Asplund, M. 2001, *Astrophys. J.*, 556, L63
- ³⁰ —. 2002, *Astrophys. J.*, 573, L137
- ³¹ Ross, M., Ree, F. H., & Young, D. 1983, *J. Chem. Phys.*, 79, 1487
- ³² Saumon, D., Chabrier, G., & Horn, H. M. V. 1995, *Astrophys. J. Suppl.*, 99, 713
- ³³ Saumon, D., & Guillot, T. 2004, *Astrophys. J.*, 609, 1170
- ³⁴ Seidelmann, K. P. 1992, ed. *Explanatory Supplement to the Astronomical Almanac* (University Science Books, Sausalito, CA)
- ³⁵ Tassoul, J.-L. 2000, *Stellar Rotation* (Cambridge University Press)
- ³⁶ von Zahn, U., Hunten, D. M., & Lehmacher, G. 1995, *J. Geophys. Res.*, 103, 22815
- ³⁷ Vorberger, J., Tamblyn, I., Bonev, S., & Militzer, B. 2007, *Contrib. Plasma Phys.*, 47, 375
- ³⁸ Vorberger, J., Tamblyn, I., Militzer, B., & Bonev, S. 2007, *Phys. Rev. B*, 75, 024206 and references therein
- ³⁹ Zharkov, V. N., & Trubitsyn, V. P. 1978, *Physics of Planetary Interiors* (Pachart Publishing House, Tucson)
- ⁴⁰ Schneider, J., the *Extrasolar Planets Encyclopaedia* <http://exoplanet.eu>

TABLE I: Constraints on Jupiter interior structure and parameters of models based on DFT-MD EOS. Predicted conditions at the core-mantle boundary (CMB) are listed last.

| Model | Equatorial radius (km) | $J_2 \times 10^6$ | $J_4 \times 10^6$ | $J_6 \times 10^6$ | Core mass (M_E) | Mantle ice (M_E) | T (K) at CMB | P (GPa) at CMB |
|-----------------------------|------------------------|------------------------|-----------------------|---------------------|---------------------|----------------------|----------------|------------------|
| Observed | 71492 | 14696.43 ± 0.21 | -587.14 ± 1.68 | 34.25 ± 5.22 | ... | ... | ... | ... |
| Solid-body rotation | 71493 | 14718 | -620 | 37.5 | 16.7 | 2.1 | 12500 | 3800 |
| Average surface winds | 71493 | 14737 | -623 | 37.3 | 16.7 | 2.1 | 12500 | 3870 |
| Preferred model: deep winds | 71492 | 14697.14 | -586.3 | 23.9 | 16.2 | 2.1 | 12500 | 3800 |